DISCUSSION

The tabulated results indicate, perhaps surprisingly, that oil mist particles of mean size as low as 1μ exhibit a diffusivity that is only about half that for air alone in the same duct. An increase in the number of perforated plates may plausibly be expected to reduce the scale of turbulence, hence the diffusivity. Indeed, five plates in place of the original two are observed to lower the oil-mist diffusivity further by 40%.

The question of whether the oil mist particles lowered the diffusivity of the air has not been considered. The matter could be readily resolved by simultaneous injection and traversing of helium and particles. We note, however, Soo's finding that with glass beads of diameter below 250μ and loadings of less than 0.06 lb. of solid/lb. of air, the stream turbulence was not significantly affected by the presence of the particles (*4*). The present oil mist concentration at the injector slit was 0.004 lb. of oil/lb. of air.

Various modifications of the described experimental procedure are possible whereby the available ranges of particle size and density may be substantially increased. Thus, the optical density probe described by Soo, et al. (*7, 8*) can be used in connection with glass microbeads at least as large as 80μ in diameter. Radioactive particles also suggest themselves in this application, the advantage of these being that they will give an indication of concentration dependent on particle mass rather than area as in the optical case.

Although the above considerations have been confined to a particulate-gas system, they are equally applicable to a particulate-liquid system, appropriate changes being made in the instrumentation.

ACKNOWLEDGMENT

The authors are grateful to Waldo C. Burns for assistance in setting up the experimental equipment and taking numerous measurements.

NOTATION

D = diffusivity, sq.ft./sec.
t = transit time between injector and sampler, sec.
v = average axial gas velocity, ft./sec.
z = distance between injector and sampler
σ = standard deviation of concentration profile, ft.

LITERATURE CITED

1. Williams, J. C. and R. Jackson, *Proc. Symp. Interaction Fluids Particles, London*, 282, 291, 297 (1962).
2. Cooperman, P., *Air Pollution Control Assoc., Paper 66-124*, 59th Ann. Meeting, San Francisco, Calif. (1966).
3. Fuchs, N. A., "The Mechanics of Aerosols," Chapt. V, Revised Ed., MacMillan, New York (1964).
4. Soo, S. L., H. K. Ihrig, and H. F. el Kouh, *J. Basic Eng.*, **82**, 609 (1960).
5. Sinclair, D., *Air Repair*, 3, 51 (Aug., 1953).
6. Robinson, M., *J. Air Pollution Control Assoc.*, **17**, 605 (1967).
7. Soo, S. L., C. J. Trezek, R. C. Dimick, and G. F. Hohnstreiter, *Ind. Eng. Chem. Fundamentals*, 3, 98 (1964).
8. Baw, P. S. and R. L. Peskin, *Tech. Rept. 108-ME-F*, Rutgers University, New Brunswick, N. J. (1966).

Manuscript received March 26, 1968; revision received May 13, 1968; paper accepted May 15, 1968.

Effects of Surfactants on Mass Transfer Inside Drops

W. S. HUANG and R. C. KINTNER

Illinois Institute of Technology, Chicago, Illinois

A model is presented to account for reduced mass transfer to drops falling through a continuous phase which contains a surface active agent. The fluid flow patterns are essentially laminar. The reduction in mass transfer is said to be due to a reduction in available interfacial transfer area and to changes in both velocity and pattern of internal circulation. These are shown to be functions of contact time and can be characterized. Experimental values agreed with the theoretically predicted ones with a deviation of less than 10%.

The transfer of heat, mass, and momentum between a continuous phase and drops of a dispersed phase is important in numerous industrial operations. Fractionation, liquid-liquid extraction, and two-phase reactions are common examples. The operations employ streams or clouds of drops, but a fundamental understanding of the effect of each variable on the behavior of a single drop is necessary for an understanding of the performance of multidrop systems. Many investigators have studied various aspects of the transfer mechanism and drop mechanics involved in

W. S. Huang is with Texaco Inc., Bellaire Research Laboratories, Bellaire, Texas.

this area. Mass transfer in the dispersed phase, in the continuous phase, or at the interface has been investigated both analytically and experimentally. However, each particular theory only partially fitted the experimental data, which exhibited considerable discrepancy. One cause of the deviations was finally realized by investigators during the last two decades. The surface active material tends to stay at the interface and affects the hydrodynamic behavior of the phases. This surface active material can be surfactants, impurities, plasticizer from the tubing used in the equipment, or metallic colloids from pipes and fittings. Wherever such material enters the situation, the data exhibit an erratic pattern. It has been observed that surfactants reduce the internal circulation of a liquid drop until it finally becomes stagnant. Consequently, mass transfer rate changes.

The reduction in mass transfer rate due to the presence of surfactants and other impurities has been reported by many investigators (*4, 5, 16, 19, 20, 31, 38, 46, 59, 60*). But there is no satisfactory theory to explain the role of surface active agents which can segregate in the interfacial layers. This work attempts to evaluate their effects on mass transfer to a drop falling through a stationary liquid field.

MASS TRANSFER MODELS

The dispersed phase resistance has been analyzed on the basis of three mathematical models. One of these, developed by Newman (*49*), is based upon a rigid sphere with no internal motion and leads to the expression

$$E_m = \frac{c_0 - c_f}{c_0 - c^*} = 1 - \frac{6}{\pi^2} \sum_{n=1}^{\infty} \frac{1}{n^2} \exp\left[- n^2 \pi^2 \frac{\mathcal{D}_D t}{a^2} \right] \tag{1}$$

When resistance to transfer in the continuous phase is zero and a laminar circulation pattern which can be described by the Hadamard (*25*) streamlines is present, the equation of Kronig and Brink (*42*) can be applied

$$E_m = 1 - \frac{3}{8} \sum_{n=1}^{\infty} A_n^2 \exp\left[- \lambda_n \frac{16 \mathcal{D}_D t}{a^2} \right] \tag{2}$$

Handlos and Baron (*28*) superimposed a turbulence due to random radial motion upon a circulatory pattern. This model yields, for zero resistance in the continuous phase,

$$E_m = 1 - 2 \sum_{n=1}^{\infty} A_n^2 \exp\left[- \frac{\lambda_n U t}{128 \left(1 + \frac{\mu_d}{\mu_c} \right) d} \right] \tag{3}$$

The numerical values of A_n and λ_n in Equations (2) and (3) are not identical. Previous workers (*6, 21, 39, 45, 56*) have used these three theoretical models, combined with one of the various empirical equations for the continuous phase resistance, to correlate droplet mass transfer data. Angelo, Lightfoot, and Howard (*2*), and Rose and Kintner (*50, 51*) have modified these approaches for oscillating spheroidal drops moving at high Reynolds numbers by the introduction of the concept of interfacial area stretch.

PREVIOUS WORK

The literature on surface active agents and their effects in bubble and drop phenomena is too voluminous for detailed review in the present case. The results of numerous workers in this field may be summarized as follows:

1. If a surface active agent be added to either phase of a dispersed fluid-fluid system, the rate of mass transfer across the phase boundary will be markedly reduced from the rate associated with chemically pure phases. (*4, 5, 16, 17, 19, 20, 22, 31, 37, 38, 40, 46, 47, 54, 57, 59, 60.*)

2. Any oscillations or other surface disturbances are damped by the presence of surfactants in the surface layers (*5, 10, 11*).

3. Colloidal materials also act as surface active agents, accumulate on the interface, are swept to the rear by convective movement and produce the same results as soluble surfactants (*10, 11, 24, 32, 33*).

4. The surfactant which arrives at the fluid-fluid interface is swept to the rear by convective motion. It accumulates in a layer forward from the rear stagnation point. This results in a spherical cap, the forward edge of which progresses toward the equator of the drop as surfactant continues to accumulate (*19, 32, 33, 53*). At the forward edge of this cap the circumferential streaming motion of the interface stops (*53*). This results in a boundary layer separation (*32, 33, 43, 53*).

5. The Hadamard (*25*) circulation pattern has a stagnation ring at the equatorial plane and at a distance of $0.707a$ from the center of the fluid sphere. This stagnation ring migrates toward the front stagnation point as surfactant accumulates on the rear surface of the fluid sphere (*19, 32, 33, 53*).

6. The drag force is higher for a dispersed fluid particle moving through a fluid field if a surfactant be added to either phase. (*18, 53.*) From the derivation of Savic (*53*) the total drag on the sphere is

$$F_D = -4\pi \mu_c a U X_2 \tag{4}$$

where X_2 is the first coefficient of the expansion in solving Gegenbauer polynomials.

7. The gross terminal velocity of a gas bubble or liquid drop moving vertically under the influence of gravity through a liquid field is greatly reduced upon the addition of a small amount of surface active agent to either phase. (*3 to 5, 10, 11, 17, 19, 23, 25, 32, 33, 41, 43, 44, 47, 53, 54, 57.*) For the case in which adsorption or desorption of the surfactant governed the surface concentration, Levich (*43*) solved for the terminal velocity and for the velocity at the equator, obtaining

$$U = \frac{2}{3} \left[\frac{g a^2 (\Delta\rho)}{\mu_c} \right] \left[\frac{\mu_d + \mu_c + \gamma_1}{2\mu_c + 3\mu_d + 3\gamma_1} \right] \tag{5}$$

$$u_\theta = \frac{1}{3} \left[\frac{g a^2 (\Delta\rho)}{2\mu_c + 3\mu_d + 3\gamma_1} \right] \tag{6}$$

in which

$$\gamma_1 = \frac{2\Gamma_0}{3\delta a} \cdot \frac{2\partial}{\partial \Gamma} \tag{7}$$

He called γ_1 a retardation coefficient.

8. Equilibrium of adsorption has been assumed to be attained before the moving fluid sphere reaches a steady state (*43, 54*). For a specified concentration of surfactant in the continuous phase, C_s, there can be only one equilibrium value for the surface concentration, Γ_0, which is the Langmuir adsorption isotherm value

$$\Gamma_0 = \frac{kC_s}{1 + \frac{kC_s}{\Gamma_\infty}} \tag{8}$$

in which k is a constant and Γ_∞ is the value of Γ_0 when $C_s \rightarrow \infty$. But this conflicts with the assumption of a gradient in concentration along the interface.

9. The segregation of the surface active agent at the interface results in a quasirigid interfacial barrier (interfacial

resistance) to mass transfer across the phase boundary (*1, 16, 19, 46, 52, 59*).

10. As the segregated surfactant in the fluid layers near the interface is swept to the rear, a high concentration results at that location. The interfacial tension at that point should be lower than at the front of the fluid sphere. It has been concluded that this results in a continuous concentration gradient along the interface (*9, 12, 14, 43, 47, 54*). The concept has been refuted by Savic (*53*) and is rejected in our work.

11. The interfacial tension is lowered by the addition of a small amount of surfactant to either phase (*9, 12, 14, 18, 24, 41, 43, 44, 47, 54*).

12. If the drag of the drop varies as surfactant accumulates on the rear surface, the fall velocity must be a function of contact time and is therefore not constant (*19, 32, 33, 53*).

13. The addition of a minute amount of a surface active agent to either phase results in a lowered internal circulation rate (*25*) for the dispersed phase (*5, 12, 16, 18, 19, 23, 32, 33, 43, 48, 53, 54, 60*). There is also a radical change in the circulatory pattern inside the drop phase.

DEVELOPMENT OF THE MODEL

The basic differential equation for mass transfer across any plane surface is:

$$\frac{dN}{dt} = KA_i\Delta c \tag{9}$$

For a circulating drop with surfactant in the continuous phase (as discussed in the previous section), a thick monolayer of surfactant accumulates in the rear of the drop and the circulation changes both in pattern and in velocity.

It has been observed by Hutchinson (*37*), Garner and Hale (*16*), and Davies and Mayers (*8*) that a layer of surfactant at the interface creates a barrier through which the solute must pass. They found that the mass transfer could be reduced to as little as 20% of that with the clean interface. If this applies to a drop with surfactant in the rear part, the mass transfer rate for the frontal part of the drop which remains circulating is approximately 2.5 times (*6, 42*) greater than that of a stagnant drop with a clean interface. Since the stagnant portion of the drop has surfactant on the interface, it further retards the mass transfer rate. It is therefore quite reasonable to assume that there is almost no mass transfer in the rear portion of the drop that is covered by surfactant. The mass transfer rate, therefore, becomes smaller as more surfactant accumulates.

For a fully circulating drop, convective mass transfer dominates the transfer phenomena. As the circulation slows down, so does the mass transfer rate. The changing pattern of circulation, that is, the migration of the stagnation ring to the axis of the drop, reveals that the volume of the circulating fluid becomes smaller as more surfactant accumulates. The circulation volume defined by Hughes and Gilliland (*36*) is the volumetric flow rate of the fluid passing through the stagnation ring. The stagnation ring becomes smaller as the circulation velocity becomes smaller. Hence, the circulation volume becomes smaller, too. If one defines a dimensionless circulation volume, that is, the circulation volume of a drop with surfactant to that of a drop without surfactant, it is not hard to visualize that the dimensionless circulation volume gives the degree of circulation which covers both effects (change in the circulation pattern and its slowing down). Since circulation is a predominant factor in mass transfer, it is reasonable to assume that the dimensionless circulation volume $[Q(t)]$ affects the mass transfer coefficient. It serves as a correction factor for the value of the mass transfer coefficient. When the drop is free from surfactants, the dimensionless circulation volume is unity. As surfactant accumulates, it varies between one and fractions. This depends on how the surfactant is adsorbed. It would be easier to understand in terms of equations.

Rewriting Equation (9) for dispersed phase resistance:

$$\frac{d(cV)}{dt} = k_d\ A_i\ (c - c^*) \tag{10}$$

By substituting for A_i and V in Equation (1), one can simplify the equation and integrate it. After substituting the limits, one obtains:

$$\ln\frac{c_f - c^*}{c_0 - c^*} = \frac{3k_d t_R}{a} \tag{11}$$

or

$$k_d = \frac{a}{3t_R}\ln\frac{c_f - c^*}{c_0 - c^*} \tag{12}$$

where k_d is the average mass transfer coefficient over the residence time t_R and c is an average concentration in the drop.

Kronig and Brink (*42*) had analyzed the mass transfer from a droplet with resistance completely in the drop phase as shown in Equation (2).

Substituting Equation (2) into (12), the mass transfer coefficient for a fully circulating drop is:

$$k_d = \frac{a}{3t_R}\ln\left\{\frac{3}{8}\sum_{n=1}^{\infty} A_n{}^2 \exp\left(-\lambda_n\frac{16\mathcal{D}t_R}{a^2}\right)\right\} \tag{13}$$

For a drop containing surfactant, the transfer area is no longer a constant. It is $4\pi a^2 - f_1(t)a^2$ where $f_1(t)a^2$ is the area covered by surfactant, which is a function of time. Hence, the area available depends on the kind of mechanism by which the drop adsorbs the surfactant. The method used to determine the adsorption mechanism and the area covered by surfactant will be discussed later.

The mass transfer coefficient for a drop containing surfactant would be $k_d[Q(t)]^n$ where $Q(t)$ is the dimensionless circulation volume and n is a number to be determined. The function $[Q(t)]^n$ is empirical, its form being suggested from the data of Horton, et al. (*33*) on the slowing of the centerline velocity with time. Values of $Q(t)$ vs. t are listed in Table 1. By rewriting Equation (9), one obtains

$$V\frac{dc}{dt} = k_d[Q(t)]^n\ [4\pi a^2 - f_1(t)a^2]\ (c - c^*) \tag{14}$$

By separating variables, one gets

$$\frac{dc}{c - c^*} = \frac{3k_d[Q(t)]^n\ [4\pi a^2 - f_1(t)a^2]\ dt}{4\pi a^3} \tag{15}$$

For a fixed value of t_R, k_d is a constant; hence, one can easily integrate Equation (15) and obtain:

$$\ln\frac{c_f - c^*}{c_0 - c^*} = \frac{3k_d}{4\pi a^3}\int_0^{t_R}[Q(t)]^n\ [4\pi a^2 - f_1(t)a^2]\ dt \tag{16}$$

or

$$E_m = 1 - \exp\left[-\frac{3k_d}{4\pi a^3}\int_0^{t_R}[Q(t)]^n\ [4\pi a^2 - f_1(t)a^2]\ dt\right] \tag{17}$$

In Equation (17) only $[Q(t)]^n$ and $f_1(t)$ are to be determined.

TABLE 1. AVERAGE DROP AGES, STAGNATION RINGS AND DUST CAP POSITION SLOW DOWN AND DIMENSIONLESS CIRCULATION VOLUME FROM HORTON'S FILM

Drop ages (min.)	Center of stagnation ring x	y	Cap position x	y	Circumference	$1-y$	Area	$\frac{v_y}{U}$	Dimensionless circulation volume $4\left(\frac{x}{a}\right)^2\frac{v_y}{U}=Q$
0	0.707	—0	0	1.0	0	0	0	0.5	1.0
2	0.719	—0.114	0.675	0.735	4.24	0.265	1.66	0.364	0.755
4	0.671	—0.296	0.86	0.51	5.40	0.49	3.08	0.28	0.426
8	0.558	—0.503	0.987	0.15	6.2	0.85	5.34	0.19	0.236
12	0.498	—0.546	0.995	0.03	6.25	0.97	6.1	0.15	0.149
16	0.509	—0.527	1.0	0	6.28	1.0	6.28	0.125	0.129
20	0.493	—0.556	1.0	0	6.28	1.0	6.28	0.112	0.117

Dimensionless Circulation Volume

The circulation volume is defined as the flow through the stagnation ring. For a fully circulating drop, it can be briefly derived as follows (35):

$$Q' = \int_0^{a/\sqrt{2}} 2\pi r v_{\theta d}\big|_{\theta=\pi/2}\, dr$$

$$= 2\pi \int_0^{a/\sqrt{2}} r\left[\left(\frac{r}{a}\right)^2 - \frac{1}{2}\right]\frac{U\mu_c}{\mu_c+\mu_d}\, dr$$

$$= \frac{\pi a^2}{8}\,\frac{U}{1+\frac{\mu_d}{\mu_c}} \qquad (18)$$

where Q' is the amount of fluid circulating per unit time. For a small viscosity in the dispersed phase, that is, $\mu_d/\mu_c \to 0$;

$$Q' = \frac{\pi a^2 U}{8} \qquad (19)$$

The maximum circulation velocity along the axis of the drop with $\mu_d/\mu_c \to 0$ in the case of full circulation is

$$v_{\max} = \frac{U}{2} \qquad (20)$$

This is the maximum circulation velocity for Hadamard's model.

If one defines an average circulation velocity, $\bar{v}$, then:

$$Q' = \frac{\pi a^2}{2}\,\bar{v} = \frac{\pi a^2}{8}\,U = \frac{\pi a^2}{4}\,v_{d\max} \qquad (21)$$

Therefore,

$$\bar{v} = \frac{v_{d\max}}{2} \qquad (22)$$

The circulation velocity for the system of a mixture of tetrachloroethylene and normal butyl benzoate in a field fluid of 96% glycerol solution was measured by Fritsch (13). The original data were taken by Horton (32) with still photographs. The slides of those photographs of different aged drops were re-examined. The surfactant that the drop accumulated in Horton's work was presumed to be colloidal material from aluminum piping. It is believed that no matter what kind of surfactant is present in the continuous fluid or how the surfactant gets into the drop, it is irrelevant to the relationship between the circulation volume and the area of the surfactant. In other words, the circulation volume (which includes the slow down in circulation and the change in circulation pattern) always has a fixed relationship with surface area covered by surfactant. The stagnation ring, the surfactant area, and the circulation velocity were measured. The drops were normalized with the radius equal to one unit and the dimensionless circulation volumes were calculated. They are tabulated in Table 1.

The surface area covered by surfactant was measured by an azimuthal angle from the center of the drop, and the circumference of the surfactant was calculated.

The relationship between the area covered by surfactant and its circumference can be worked out easily using the geometry of a sphere. The surface area covered by surfactant for a drop with a unit radius,

$$f_1 = 2\pi(1-r_1) \qquad (23)$$

where r_1 is the dimensionless radius r.

The circumference of surfactant for a drop with a unit radius,

$$C_{m1} = 2\pi\sqrt{1-r_1^2} \qquad (24)$$

From Equations (23) and (24) the relationship between C_{m1} and f_1 is

$$C_{m1} = \sqrt{(4\pi - f_1)f_1} \qquad (25)$$

If one knows the area, the circumference of surfactant can be obtained from Equation (25). The dimensionless circulation volume as a function of time is listed in Table 1. The circumference of the surfactant on a drop was plotted as a function of time from which the relationship between the dimensionless circulation volume and the circumference of surfactant was obtained. This curve can be fitted by an equation as

$$Q(t) = 0.4(6.2832 - C_{m1})^{0.46} + 0.071 \qquad (26)$$

where C_{m1} is the circumference of surfactant on a drop with a unit radius. It is obtained by knowing f_1, the area of a unit-radius drop covered by surfactant, as shown in Equation (25). It was found in Horton's films that the surfactant would hardly go beyond the equator of the drop, even though the drop had a long residence time in the continuous phase.

The dimensionless circulation volume approaches 0.071 as surfactant covers the entire hemisphere of the drop. The circulation is so slow that more than half of the drop is stagnant. From Equations (1), (2), and (12), one can calculate the ratio of the mass transfer coefficient of a circulating drop to that of a stagnant drop. The simple calculation reveals that the mass transfer of a circulating drop is twice that for stagnant drop of the same size. This results in a lower limit of the correction factor $[Q(t)]^n$. The value of $[Q(t)]^n$ cannot be smaller than 0.5. If it is, it means that the mass transfer coefficient for a partially circulating drop is smaller than that for a completely stagnant drop, which is considered impossible.

With this in mind, the value of n could be obtained easily by assuming that the mass transfer coefficient for a

drop with less than one tenth of its volume circulating approaches the mass transfer coefficient for a stagnant drop. The value n obtained in this manner is equal to 0.2. This keeps the variation of $Q(t)$ above 0.5.

From Equations (25) and (26), $Q(t)$ can be obtained, if $f_1(t)$ is determined. The next section is devoted to the method used to find f_1 as a function of time.

An indirect method that measured the instantaneous velocity of the fall of a drop was used to determine the amount of surfactant in the rear of the drop. The terminal velocity for an uncontaminated drop with $\mu_d/\mu_c \to 0$ can be derived from Hadamard's solution (35) as:

$$U = \frac{(\rho_d - \rho_c) g a^2}{3\mu_c} \tag{27}$$

Savic (53), who studied the circulation of drops with surfactants, arrived at an equation for the drag force on a drop with $\mu_d/\mu_c \to 0$ as follows:

$$F_D = -4\pi\mu_c U a X_2 \tag{4}$$

where X_2 is a function of θ_0, which is the azimuthal angle of the uncontaminated surface.

When the drop reaches its terminal velocity, the action of gravity is balanced by the drop's viscous drag, that is,

$$\frac{4}{3}\pi a^3 (\rho_d - \rho_c) g = -4\pi\mu_c U a X_2 \tag{28}$$

Rearranging the equation above, one obtains:

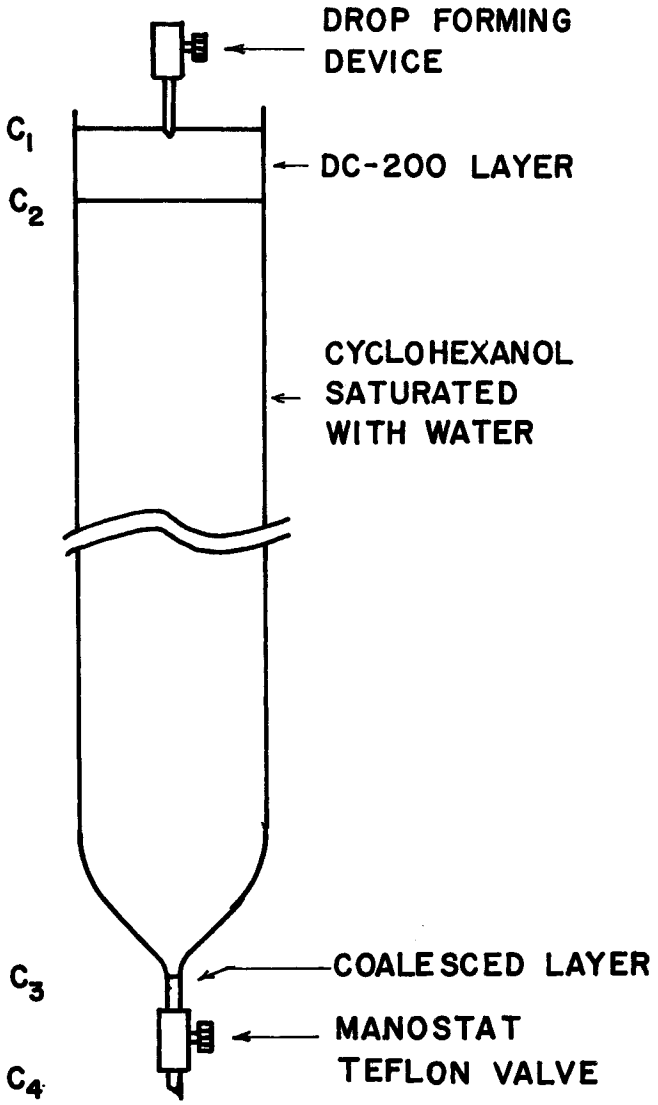

Fig. 1. Extraction apparatus.

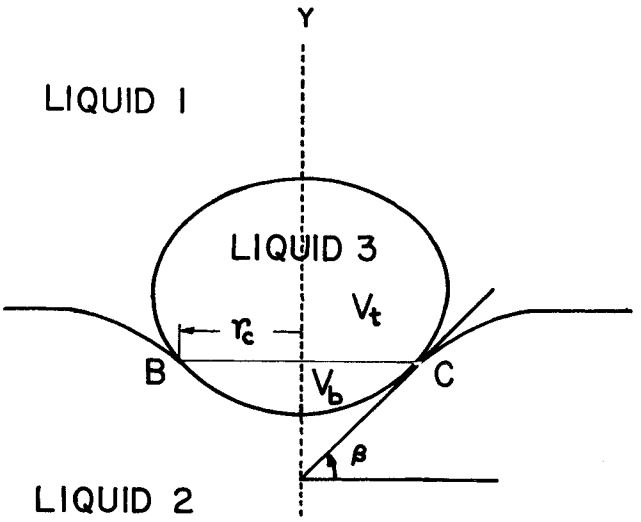

Fig. 2. Liquid drop staying at the interface between two other liquids.

$$U = -\frac{(\rho_d - \rho_c) g a^2}{3\mu_c X_2} \tag{29}$$

The difference between Equations (27) and (29) is the coefficient X_2 which varies from -1 for a fully circulating drop to -1.5 for a completely contaminated drop. X_2 is plotted against the azimuthal angle, which shows how much of the surface is covered by surfactant.

Hence, if one can measure the instantaneous fall velocity of a drop in a continuous phase containing surfactant, the area of the drop covered by surfactant can be obtained from the ratio of the contaminated drop's instantaneous velocity to the velocity of the same drop without surfactant. The ratio is X_2, which tells how much surface is covered by surfactant in that particular instant. If enough data are taken, then the history of how the surfactant accumulated in the rear of the drop can be obtained. This, in turn, tells one through Equations (25) and (26) what the circulation pattern and circulation volume are at that particular moment. If one can fit the change in area covered by surfactant, f_1, as a function of time, one can substitute this into Equations (25) and (26) and integrate Equation (17).

EXPERIMENTAL

Choice of System

To test the model developed above, an experimental system that meets all the assumptions made in the development of the model must be set up. A system of cyclohexanol and water was used. Cyclohexanol and water are partially miscible liquids. In this experiment, cyclohexanol saturated with water was used as the continuous phase and pure water droplets were used as the dispersed phase. Hence, when water droplets fell through the continuous phase, only transfer of cyclohexanol from the continuous phase to the pure water droplets occurred. The transfer of water to the continuous phase was prohibited. Since the continuous phase was saturated with water, the mass transfer resistance lay entirely inside the drop phase. This was the condition assumed in the model. The above technique was first employed by Colburn and Welsh (7) and has subsequently been used by many other investigators (*15, 21, 26, 30, 58*) to measure the individual film resistance of one phase.

Materials

First grade chemically pure cyclohexanol was used without further purification, since an arbitrary surfactant would be added to the cyclohexanol phase before the mass transfer experiment took place. Laboratory distilled water was freshly redistilled before each use so that the dispersed phase was as-

sumed to be free of surfactant. Ocenol and Zonyl S-13 were used as surfactants. Ocenol which contains mainly oleyl alcohol and is rich in cetyl and unsaturated C_{16} alcohols, is soluble in cyclohexanol and insoluble in water. Its average molecular weight is about 255. Zonyl S-13 is a fluorochemical surfactant composed of 100% fluoroalkyl phosphate free acid. It is a soft waxy solid which dissolves readily in cyclohexanol solution but is insoluble in water at room temperature.

The physical properties of interest in this work are density, viscosity, interfacial tension, mutual solubility, and diffusivity. The density, viscosity, and mutual solubility were measured and plotted as a function of temperature (*35*). A Cenco du Nouy ring tensiometer model 70545 was used to measure the interfacial tension between water and cyclohexanol saturated with water.

The Wilke-Chang (*61*) correlation was used to predict the diffusivity of cyclohexanol into water.

Apparatus

The Drop-Forming Device: A 10 ml. microburet was fitted with a Manostat Teflon needle valve. Various size nozzles can be fitted in the other side of the valve, so that an adequate size drop could be formed. To produce a constant drop size, a constant head had to be maintained. This was done by tightly fitting the top of the buret with a rubber stopper through which an open capillary tube was inserted. This maintained a constant head inside the buret as long as the water level was higher than the end of the capillary. The buret was then recalibrated.

The nozzle was made by heating the glass tube over a propane torch until a small capillary about 0.05 mm. in diameter was drawn. The capillary was cut to form a nozzle.

The Extraction Column: Three tubes 3½ in. in diameter and 6, 12, and 22 in. long were used as an extraction column. The bottom of the column was conical in shape, with the outlet an 0.5 cm. diam. tube about 1 in. long. The tube was connected to a Manostat Teflon valve, so that the flow rate could be controlled. The columns were carefully mounted on a steel frame and kept vertical.

Mass Transfer

A layer of Dow Corning 200 fluid (abbreviated DC 200) was carefully poured from the beaker to the continuous phase after it was filled in the extraction column.

The drop-forming device described in the previous section was placed along the center line of the column with the nozzle exactly 1 in. from the continuous phase, as shown in Figure 1.

After everything was set up, the Manostat valve was adjusted so that drops of the desired size were formed. They usually ranged from 0.2 to 0.3 cm. in diameter. When the drops arrived at the bottom, they coalesced in the small connecting tube above the Manostat valve. When the level of the coalesced layer went up, the Manostat valve was carefully opened so that the coalesced layer was always maintained at the same level and did not go beyond the connecting tube. The first few drops of water from the Manostat valve were discarded because of possible contamination from the continuous phase which had been trapped in the bottom of the tube and could not be replaced by the coalesced layer. The rest was collected in the manner described above so that the coalesced layer was always maintained at the same level. The sample was collected in a small test tube ready for analysis.

Referring to Figure 1, the concentration of the drop withdrawn from valve c_4 could be analyzed; but concentration c_2, the concentration of the drop before it entered the continuous phase, could not be evaluated.

An approximate method was used to run the extraction experiment in the DC 200 layer. This method was the same as those in the previous experiment, except that a shorter column was used. The nozzle tip and the coalesced layer were kept 1 in. apart. And the dispersed phase was withdrawn as fast as possible. Hence the concentration here could be assumed to be the same as c_2.

Experiments were run in the 12 and 22 in. columns and the surfactant concentrations were 0.1% of Ocenol, and 0.1 and 0.175% of Zonyl S-13.

Gas Chromatography

The samples were analyzed in an Aerograph model 90-P3 gas chromatograph. A 5 ft. stainless steel column of 10% Carbowax 20 M on Chromosorb T was used for the separation of water and cyclohexanol. The carrier gas was high purity helium.

Instantaneous Fall Velocities

Since the speed of the drops was slow, a movie camera speed of 32 frames/sec. was fast enough to investigate the instantaneous falling velocity. The extraction column and drop-forming device were operated as before. To obtain better contrast, a tracer of blue dye was added to the drop phase. A cine-Kodak K-100 camera with Eastman Tri-X 7278 reversal film was used. The distance from the center of the column to the lens of the camera was 4 ft., and the speed of the camera was set at 32 frames/sec. Beside the column there was an electric chronograph that divides a second into 100 divisions. A transparent scale was cemented on the wall of the column. Therefore, the drop position could be recorded as a function of time in the film, and from this the instantaneous drop velocity could be determined. The temperature of the continuous phase was recorded when the movie was taken. This was used to calculate the theoretical fall velocity.

Complete experimental data are contained elsewhere (35).*

DISCUSSION OF RESULTS

Fluid Drop Going Through Fluid-Fluid Interface

When DC 200 was used as an upper layer for the continuous phase to eliminate the end effects, it brought up the problem of a liquid drop going through the liquid-liquid interface. How does the drop behave when it passes through the interface of two other liquids? This is similar to the problem of the mechanism of a heavy liquid drop falling into a light liquid and coalescing with the heavy one. The only difference is that, in the coalescence problem, after the drop passes through the interface it coalesces with the bottom layer, while in this case the drop keeps going. Many investigators studied the coalescence of droplets of heavy liquid in a medium or light liquid. They developed many theories about a drop approaching the interface, the drop at the interface, and the rupture of the film. In this work, we are most interested in what happens when a drop is going through the interface. A force balance around the free surface of the drop and the interface at the moment when the drop was about to pass through the interface was shown as follows (see Figure 2):

$$\rho_3(V_t + V_b)\frac{g}{g_c} - (\rho_1 V_t + \rho_2 V_b)\frac{g}{g_c} = 2\pi r_c \sigma \sin\beta - \Delta p_\sigma \pi\ r_c^2 \quad (30)$$

where Δp_σ is the capillary pressure induced by the curved interface. Δp_σ is defined as follows:

$$\Delta p_\sigma = \sigma\left[\frac{1}{R_1} + \frac{1}{R_2}\right] \quad (31)$$

where R_1 and R_2 are the principal radii of curvature at C. If the left-hand side of Equation (30) is much greater than the right-hand side, there is no problem when the drop passes through the interface. If the left-hand side is much smaller than the right-hand side, the drop will stay at the interface.

There were many theories about the thinning of the film between the drop and liquid 2. When the film reached a certain thickness, it would rupture. The time required for

* Table 2 has been deposited as document NAPS-00485 with the ASIS National Auxiliary Publications Service, c/o CCM Information Sciences, Inc., 22 W. 34th St., New York 10001 and may be obtained for $1.00 for microfiche or $3.00 for photocopies.

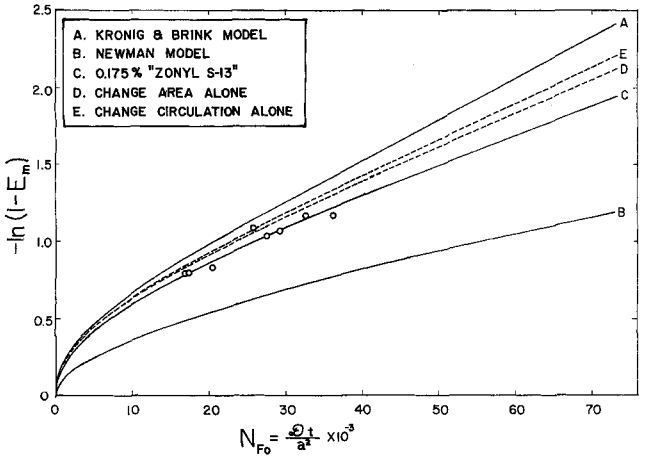

Fig. 3. —ln $(1-E_m)$ vs. Fourier number for 0.1% Ocenol.

a drop to break up the film after it arrived at the interface was called the breakup time. It was found by many investigators (*34, 29*) that the breakup time is statistical in nature. This was confirmed in this experiment, too.

After the drop went through the interface, it resumed its natural behavior, depending on the relative densities and viscosities of the dispersed and continuous phases. When some drops containing blue dye were passed through the interface, it was found that circulation started right after a drop left the interface. As far as mass transfer is concerned, the time that a drop stays at the interface is immaterial. Mass transfer will not occur in the continuous phase until the drop breaks through the interface.

Monolayer of Surfactants in the Rear of the Drop

The mass transfer model in this work assumes that a monolayer of surfactant accumulates in the rear of the drop. This contradicts the prevailing model of a concentration gradient of surfactant on the drop surface. Actually, the concentration gradient around the surface is very hard to believe if one has seen the dust cap in the rear of the drop (*35*).

Theoretically, a uniform layer of surfactant could be formed in the following manner: As the surfactant reaches the surface of the drop, it is swept to the rear of the drop by the tangential velocity on the surface. For a drop 0.2 cm. in diameter having a Reynolds number of about 1 (for example, the system used in this work), the tangential velocity is about 0.4 cm./sec. at the equator of the drop, and becomes slower near the rear of the drop. The first molecule of surfactant stays at the rear pole where the tangential velocity is zero. The molecules of surfactant that come later can only go next to the previous molecule. They are forced to stay in this position by the constant drive of the tangential velocity. This process continues as the drop falls. The surfactant layer that grows in this manner has to be a uniform layer. The only possibility that could cause a concentration gradient on the surface is molecular diffusion of the surfactant molecules themselves in the direction countercurrent to the tangential velocity.

The diffusivity of the large surfactant molecules through the continuous phase is of the order of 10^{-5} sq.cm./sec. (*43*). Consider a tiny stream tube in the continuous phase very close to the interface and at the equatorial plane. The speed of travel (the velocity component of the diffusional flux) of the surfactant molecules can be shown to be of the order of 10^{-4} cm./sec. The opposing convective velocity of the fluid in the stream tube near the interface is about 0.4 cm./sec. A concentration gradient of surfactant can not be maintained along the interface due to the low order of magnitude of diffusional transport. As the surfactant layer builds up, the surface covered by the surfactant is immovable. The tangential velocity stops abruptly at the circumference of the surfactant, thereby causing the velocity vector to change in direction. This change in direction causes a boundary layer separation on the circumference of the surfactant. Close examination of the continuous phase stream line in Horton's film also confirms this. The upstream and downstream stream lines are not symmetrical to the equator of the drop, and the boundary layer separation occurs at the circumference of the surfactant layer.

The model for a concentration gradient *on the surface* of the drop did not have any experimental support. When this model was applied to the real case (*54*), it did not seem to agree with the behavior of the drop. Therefore, the existence of an interfacial tension gradient on the drop is extremely doubtful. However, the physical evidence of the homogeneous dust cap and the boundary layer separation do suggest that a clear surfactant edge exists where the tangential velocity comes to a halt and a discontinuity in the interfacial tension occurs. In most cases, the interfacial tension between the continuous phase and the dispersed phase was very low. When surfactant was added, the interfacial tension of the surface covered by surfactant became lower, but the difference was so small that the distortion of the droplet was not noticeable. In this work, the interfacial tension between the dispersed phase and the continuous phase for a surfactant-free interface was 3.46 dyne/cm., with additions of 0.1% Ocenol or 0.1% Zonyl S-13, the interfacial tension readings were 3.37 dyne/cm. The difference was so small that it was considered to be within the experimental error.

Surfactant Adsorption Mechanism

In the theoretical development of this work, the factor controlling the adsorption of the surfactant on the surface was not important. What one needs to know is how much surface is covered by surfactant at any given moment. This was determined by measuring the instantaneous falling velocity.

In all cases, it was found that a certain surface area was covered by surfactant at $t = 0$. This is not surprising if one realizes that when the drop first came into contact with the solution containing surfactant, the surfactant would stay in the interface immediately. Because of the motion of the drop through the interface of the top layer and the continuous phase, the surfactant would be swept to the back of the drop. There was another possibility, that is, the DC 200 layer on the top of the continuous phase might act as a surfactant. When the drop passed through it, a thin layer of DC 200 might wrap around the drop. As the drop went through the interface, the thin film would break up. Some of the DC 200 might go with the drop through the interface and form a small dust cap. This is probably

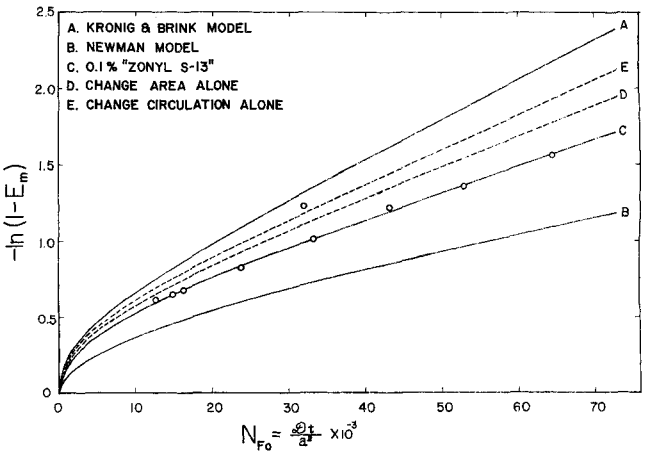

Fig. 4. —ln $(1-E_m)$ vs. Fourier number for 0.1% Zonyl S-13.

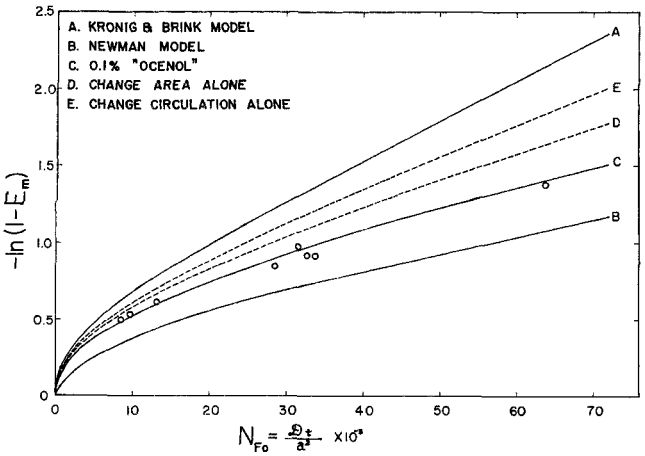

Fig. 5. —ln $(1-E_m)$ vs. Fourier number for 0.175% Zonyl S-13.

a more reasonable explanation.

From the data, it seemed that the area covered by surfactant was a linear function of time. Because of the difficulty of getting data from motion picture film, this approximation was believed good enough. For drops that fell farther than 40 cm. (the distance recorded with the motion picture film), a linear extrapolation was made. This extrapolation remained to be proved in a longer column. A camera that takes more than 40 ft. of film without rewinding would be necessary to satisfactorily make the investigation in a longer column. Because the camera speed had to be maintained at least at 32 frames/sec. to get enough data for the instantaneous falling velocity, the camera could only photograph 40 cm. of the drop's fall. Therefore, a more sophisticated way of measuring the drop's instantaneous falling velocity was required.

Mass Transfer

A computer program to calculate Equation (17) was used (35). The adsorption mechanisms were different for different surfactants in the continuous phase. The fractional extraction and mass transfer coefficients are shown for both Kronig and Brink's model and the one used in this work.

To compare the present model with the fully circulating model of Kronig and Brink and the completely stagnant model of Newman, a computer program was designed to determine the fractional extraction, the mass transfer coefficient, and the Sherwood number in each case. The fractional extractions are plotted as $-\ln(1-E_m)$ against the dimensionless time group, $\mathcal{D}t/a^2$, which is known as Fourier Number, in Figures 3, 4, and 5. In the system containing 0.1% "Ocenal", the fractional extraction was between those of the fully circulating drop and the stagnant drop. (See Figure 3.) This was expected because of the contamination of the surfactant. With 0.1% Zonyl S-13 as the surfactant, the curve was close to that for the stagnant drop. (See Figure 4.) This indicates that the surfactant accumulated so fast that the reduction in the mass transfer area and the reduced circulation made the mass transfer rate of the drop slow. For the continuous phase containing 0.175% Zonyl S-13 (Figure 5), the accumulation was even faster, because of the higher surfactant concentration in the continuous phase. Hence the mass transfer rate was slower.

The Sherwood number was also plotted against dimensionless time for each case. (See Figures 6 to 8.) The tendencies were similar to those shown by the fractional extractions.

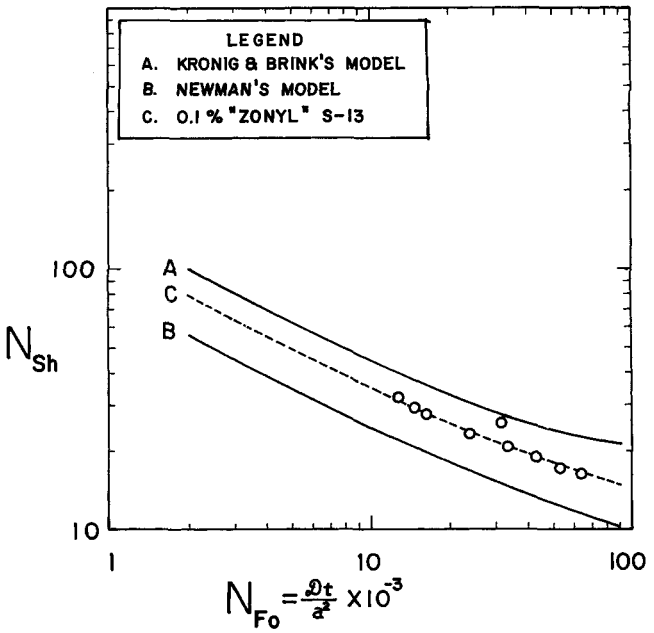

Fig. 7. Sherwood number vs. Fourier number for 0.1% Zonyl S-13.

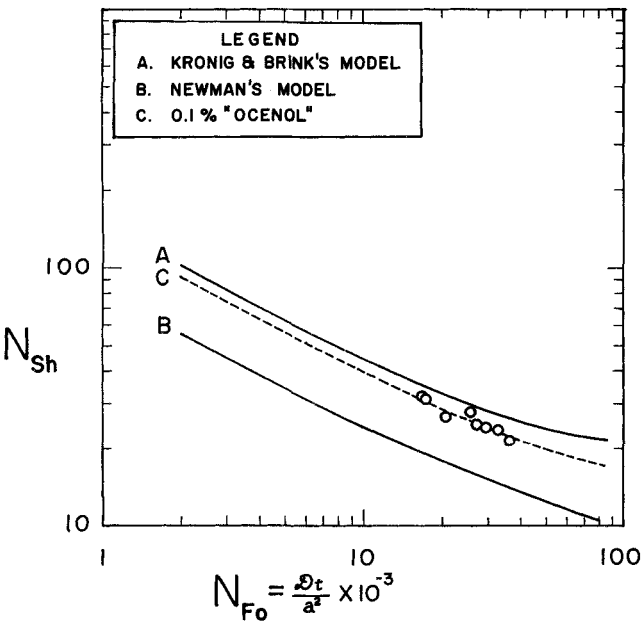

Fig. 6. Sherwood number vs. Fourier number for 0.1% Ocenol.

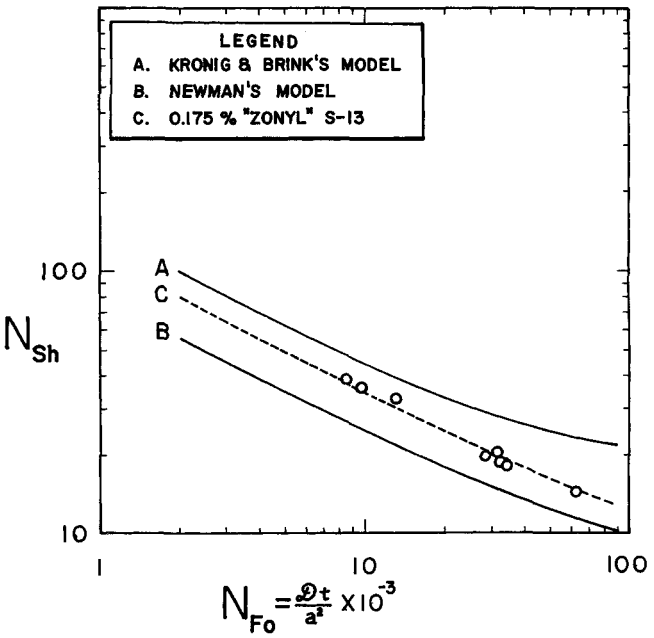

Fig. 8. Sherwood number vs. Fourier number for 0.175% Zonyl S-13.

All the experimental data (in the form of fractional extractions) were compared with the theoretical values (35), and plotted in Figure 9, which showed the excellent agreement of the calculated and experimental values. The calculated Sherwood number vs. the observed Sherwood number is shown in Figure 10. Most of the data agreed within less than 10%. Most of the experimental data plotted in Figures 3, 4, and 5, are close to the predicted curve.

The reduction in circulation and the reduced transfer area were proved to be the two factors that reduced the mass transfer rate. This analysis also showed that the dimensionless circulation volume, which shows the effect of the changing circulation pattern and the slowing down of the circulation velocity, was a proper parameter to characterize the reduction of circulation in the drop for the reduction in mass transfer rate. To ignore any one of the effects would lead to a serious mistake. Computer programs that considered the change in transfer area alone and the change in the circulation alone were also written (35). The fractional extractions of these hypothetical models were plotted as dashed lines in Figures 3, 4, and 5. This comparison showed that either effect acting alone, could never explain the low mass transfer rate in the presence of surfactant. Considering only the reduction in transfer area would be closer to the real case, but the role of the reduction in circulation still could not be ignored.

This model was applicable for low Reynolds numbers at which the drop retains a perfect spherical shape. The drop viscosity should be negligible compared to the continuous phase viscosity and the resistance of mass transfer in the dispersed phase alone.

CONCLUSIONS

1. Both the reduction in mass transfer area and the slow down in the circulation are necessary to predict the low mass transfer rate with surfactant.
2. The surfactant accumulating in the rear of the drop acts as a barrier to hinder the passage of diffusing molecules. However, this effect alone could not explain the reduction in mass transfer. The present model accounts for both the barrier theory and hydrodynamic theory to explain the low mass transfer rate due to surfactant.
3. An equation has been developed to predict the fractional extraction for different systems. The adsorption mechanism of surfactant on the drop in each system has to be predetermined. Experimental results agree with the model to within a deviation of less than 10%.
4. Using a movie camera to measure the instantaneous falling velocity is feasible.
5. Savic's equation to predict the relationship between the area covered by surfactant and the instantaneous falling velocity is proved to be valid.
6. Gas chromatography is shown to be an effective and accurate method of measuring solute concentration.

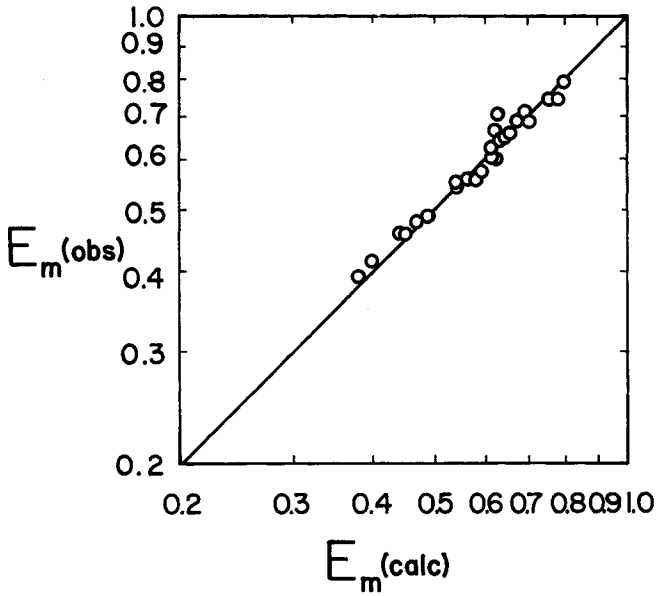

Fig. 9. Calculated and observed fraction extracted.

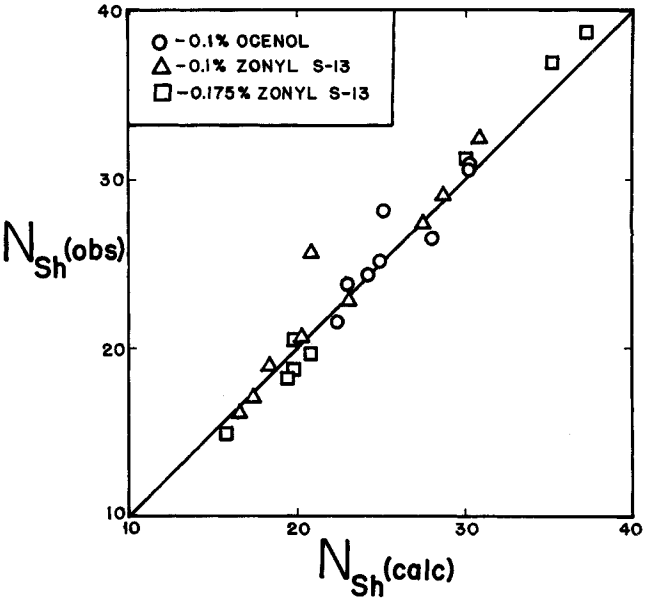

Fig. 10. Calculated and observed Sherwood numbers.

ACKNOWLEDGMENT

This work was supported by Research Grant GK-1425 from the National Science Foundation. The authors wish to thank Dr. S. E. Cremer for his aid with the chromatography and to Dr. D. T. Wasan for his review of the work.

NOTATION

a = radius of drop
A_i = interfacial area, sq.cm.
A_n = constant for Equation (2)
a = radius of a sphere, cm.
C_s = surfactant concentration in the bulk, g./100 ml.
C_{m_1} = circumference of surfactant on a drop with unit radius
c = concentration, g. mole/cc.
c_0 = initial concentration, g. mole/cc.
c_f = final concentration, g. mole/cc.
c^* = equilibrium concentration, g. mole/cc.
d = diameter, cm.
E_m = fractional extraction, $(c_0 - c_f)/(c_0 - c^*)$
F_D = total drag force on a drop, dyne/sq.cm.
f_1 = surface area of a normalized drop covered by surfactant
g = acceleration of gravity, 980 cm./sq.sec.
K = mass transfer coefficient, cm./sec.
K_d = overall mass transfer coefficient, cm./sec.
k = constant
k_c, k_d = dispersed and continuous phase mass transfer coefficient, cm./sec.
N = moles of component, g. mole
N_{Fo} = Fourier number, $\mathcal{D}t/a^2$
N_{Sh} = Sherwood number for continuous phase, $k_c d/\mathcal{D}$
P_σ = capillary pressure induced by interfacial tension,

dyne/sq.cm.
$Q(t)$ = dimensionless circulation volume
Q' = circulation volume, cc./sec.
R_1, R_2 = principal radii of curvature of a curved surface, cm.
r_c = radius defined in Figure 2
r_1 = dimensionless radius
t = time, sec.
t_R = residence time, sec.
U = velocity of the drop in a continuous medium, cm./sec.
u_θ = velocity of θ component at $\theta = \pi/2$ r = a, cm./sec.
V = volume of a drop, cc.
$\overline{v}$ = average velocity, cm./sec.
v_θ = velocity in θ direction, cm./sec.
X_n = coefficient of the Gegenbauer polynomial, $X_n = H_n' \; a^{-n+1} \; U^{-1}$

Greek Letters

β = angle defined in Figure 2
γ_1 = symbol defined in Equation (7)
Γ = surface concentration of surfactant, g. mole/sq.cm.
Γ_0 = initial surface concentration of surfactant, g. mole/sq.cm.
Γ_∞ = value of Γ_0 when $C_s \rightarrow \infty$
δ = molecules of surfactant adsorbed per unit time, $\delta = \partial P(\Gamma)/\partial\Gamma - \partial Q(\Gamma)/\partial\Gamma$
μ = viscosity, g./cm.-sec.
π = 3.14159
ρ = density, g./cc.
σ = interfacial tension, dyne/cm.
$\mathcal{D}$ = molecular diffusivity, sq.cm./sec.

Subscripts

t = top
b = bottom
c = continuous phase
d = dispersed phase

LITERATURE CITED

1. Aksel'rud, G. A., *Zh. fiz. khim.*, **27**, 1445 (1953).
2. Angelo, J. B., E. N. Lightfoot, and D. W. Howard, *AIChE J.*, **12**, 751 (1966).
3. Baird, M. H. I., and A. E. Hamielec, *Can. J. Chem. Eng.*, **40**, 119 (1962).
4. Boye-Christensen, G., and S. G. Terjesen, *Chem. Eng. Sci.*, **7**, 222 (1958).
5. *Ibid.*, **9**, 225 (1959).
6. Calderbank, P. H., and I. J. O. Korchinski, *ibid.*, **6**, 65 (1956).
7. Colburn, A. P., and D. B. Welsh, *Trans. Am. Inst. Chem. Engrs.*, **38**, 179 (1942).
8. Davies, J. T., and G. R. A. Mayers, *Chem. Eng. Sci.*, **16**, 55 (1961).
9. Davies, J. T., and E. K. Rideal, "Interfacial Phenomena," Academic Press, New York (1963).
10. Elzinga, E. R., and J. T. Banchero, *AIChE J.*, **7**, 78 (1961).
11. Elzinga, E. R., and J. T. Banchero, *Chem. Eng. Prog. Symposium Ser., No. 29*, **55**, 149 (1960).
12. Friedlander, S. K., *AIChE J.*, **3**, 43 (1957).
13. Fritsch, T. R., Unpublished report, Illinois Inst. Tech., Chicago (1962).
14. Frumkin, A. N., and V. G. Levich, *Zh. fis. khim.*, **21**, 1183 (1947).
15. Garner, F. H., A. Foord, and M. Tayeban, *J. Appl. Chem.*, **9**, 315 (1959).
16. ———, and A. R. Hale, *Chem. Eng. Sci.*, **2**, 157 (1953).
17. ———, and Hammerton, D., *ibid.*, **3**, 1 (1954).
18. Garner, F. H., and P. J. Haycock, *Proc. Roy. Soc.*, **A252**, 457 (1959).
19. ———, and A. H. P. Skelland, *Chem. Eng. Sci.*, **4**, 149 (1955).
20. ————————, *Ind. Eng. Chem.*, **48**, 51 (1956).
21. Garner, F. H., and Tayeban, M., *Anales Real Soc. Espan. Fis. Quim.*, **LVI(B)**, 476 (1960).
22. Griffith, R. M., *Chem. Eng. Sci.*, **12**, 198 (1960).
23. *Ibid.*, **17**, 1057 (1962).
24. Haberman, W. L., and R. K. Morton, David Taylor Model Basin, Rept. No. 802, U. S. Navy, Washington (1953).
25. Hadamard, J., *Compt. Rend.*, **152**, 1735 (1911).
26. Hamielec, A. E., and A. I. Johnson, *Can. J. Chem. Eng.*, **40**, 41 (1962).
27. Hammerton, D., and F. H. Garner, *Trans. Inst. Chem. Eng., (London)*, **32**, 317 (1954).
28. Handlos, A. E., and T. Baron, *AIChE J.*, **3**, 127 (1957).
29. Hartland, S., *Trans. Inst. Chem. Eng.*, **45**, 797 (1967).
30. Heertjes, P. M., W. A. Holve, and H. Talsma, *Chem. Eng. Sci.*, **3**, 122 (1954).
31. Holm, A., and S. G. Terjesen, *ibid.*, **4**, 265 (1955).
32. Horton, T. J., MS thesis, Illinois Inst. Tech., Chicago (1960).
33. Horton, T. J., T. R. Fritsch, and R. C. Kintner, *Can. J. Chem. Eng.*, **43**, 143 (1965).
34. Hsu, G. C., MS thesis, Illinois Inst. Tech., Chicago (1967).
35. Huang, W. S., Ph.D. thesis, Illinois Inst. Tech., Chicago (1968).
36. Hughes, R. R., and E. R. Gilliland, *Chem. Eng. Progr.*, **48**, 497 (1952).
37. Hutchinson, E. J., *J. Phys. Colloidal Chem.*, **52**, 897 (1948).
38. Jenkins, R., "Heat Transfer and Fluid Mechanics Institute," Stanford Univ. Press, Palo Alto, Calif. (1951).
39. Johnson, A. I., and A. E. Hamielec, *AIChE J.*, **6**, 145 (1960).
40. Johnstone, H. F., *Trans. Am. Inst. Chem. Eng.*, **35**, 621 (1939).
41. Katz, H. M., MS thesis, Univ. Cincinnati, Ohio (1950).
42. Kronig, R., and J. C. Brink, *Appl. Sci. Res.*, **A-2**, 142 (1950).
43. Levich, V. G., "Physicochemical Hydrodynamics," Prentice-Hall, Englewood Cliffs, N. J. (1962).
44. Licht, W., and G. S. R. Narasimhamurty, *AIChE J.*, **1**, 366 (1955).
45. ———, and W. F. Pansing, *Ind. Eng. Chem.*, **45**, 1885 (1953).
46. Lindland, K. P., and S. G. Terjesen, *Chem. Eng. Sci.*, **5**, 1 (1956).
47. Lochiel, A. C., *Can. J. Chem. Eng.*, **43**, 40 (1965).
48. Marsh, B. D., and Heideger, W. J., *Ind. Eng. Chem. Fundamentals*, **4**, 129 (1965).
49. Newman, A. B., *Trans. Am. Inst. Chem. Eng.*, **27**, 203 (1931).
50. Rose, P. M., Ph.D. thesis, Illinois Inst. Tech., Chicago (1965).
51. ———, and Kintner, R. C., *AIChE J.*, **12**, 530 (1966).
52. Ruckenstein, E., *Revue de Chim.*, **6**, 221 (1961).
53. Savic, P., *Nat. Res. Council Can., Rept. No. MT-22*, Ottawa (1953).
54. Schechter, R. S., and R. W. Farley, *Can. J. Chem. Eng.*, **41**, 103 (1963).
55. Sherwood, T. K., J. E. Evans, and J. V. A. Longcor, *Ind. Eng. Chem.*, **31**, 1144 (1939).
56. Skelland, A. H. P., and R. M. Wellek, *AIChE J.*, **10**, 491, 781 (1964).
57. Wasserman, M. L., Ph.D. thesis, Northwestern Univ., Evanston, Ill. (1966).
58. Wellek, R. M., Ph.D. thesis, Illinois Inst. Tech., Chicago (1963).
59. West, F. B., A. J. Herman, A. T. Chong, and L. E. K. Thomas, *Ind. Eng. Chem.*, **44**, 625 (1952).
60. ———, P. A. Robinson, A. C. Morgenthaler, T. R. Beck, and D. K. McGregor, *ibid.*, **43**, 234 (1951).
61. Wilke, C. R., and P. Chang, *AIChE J.*, **1**, 264 (1955).

Manuscript received January 26, 1968; revision received April 26, 1968; paper accepted May 23, 1968.